Dynamic polariton condensation in a single GaN nanowire-dielectric microcavity

Ayan Das, Pallab Bhattacharya, Animesh Banerjee, and Marc Jankowski

Phys. Rev. B **85**, 195321 — Published 22 May 2012

DOI: 10.1103/PhysRevB.85.195321

Dynamic Polariton Condensation in Single GaN Nanowire-Dielectric Microcavity

Ayan Das, Pallab Bhattacharya*, Animesh Banerjee and Marc Jankowski

Center for Photonic and Multiscale Nanomaterials, Department of Electrical Engineering and Computer Science, University of Michigan, Ann Arbor, Michigan 48109, USA
*Corresponding author: pkb@eecs.umich.edu, Phone: 734-763-6678; Fax: 734-763-9324

We have experimentally investigated the dynamic polariton condensation behavior in a single GaN nanowire strongly coupled to a dielectric microcavity under non-resonant optical excitation. Both time-integrated and time-resolved polariton luminescence measurements have been made in the temperature range of 25 to 100K (corresponding to exciton-cavity photon detuning of -3.0 to +4.2 meV). Polariton lasing is observed in the entire temperature range, with the lowest threshold energy of 57 nJ/cm^2 measured at 50K (δ = -1.3 meV). All the measurements indicate that at the lower temperatures, the degenerate polariton condensate is not in thermal equilibrium with the phonon bath. At 85 and 100K (δ = +2.3 and 4.2 meV) the system attains a state close to thermal equilibrium via dynamic Bose condensation. The best results are obtained at T_{latt} = 85K, for which T_{LP} = 88.8K, and this is the highest temperature recorded for an equilibrium phase transition in exciton-polariton condensates.

Microcavity exciton-polaritons, which are elementary excitations in strongly coupled exciton-photon systems, have been the subject of interest and intense research since their first observation almost two decades ago[1-3]. Research in this field with semiconductors has been driven with two interrelated goals. The first is the achievement of a coherent light source, also termed a *polariton laser*[4-9], wherein a degenerate and coherent state of exciton-polaritons is generated by a combination of polariton-phonon and stimulated polariton-polariton scattering. The coherent polariton states generate coherent light by spontaneous radiative recombination. Optically excited polariton lasers have been demonstrated with different quantum confined and nano-scale materials and microcavities[6-8,10]. While the polariton lifetime has to be comparable to the relaxation times for such lasing to occur, the system is in a metastable condensed state in which the bosonic polaritons in the degenerate condensate are only in equilibrium amongst themselves, and not with the lattice. At the other extreme is the case of a degenerate Bose-Einstein condensate in perfect thermal equilibrium with the lattice and the polariton lifetime is extremely long, leading to long-term temporal coherence and long-range spatial coherence[11-13]. In real systems, the polaritons have a finite lifetime, which is rather short. However, by engineering the polariton dynamics and the temperature it is possible to achieve dynamic condensation, where the system can attain a state close to thermal equilibrium. The exciton-cavity detuning δ plays an important role in contributing to the kinetics and the thermodynamics of strongly coupled systems[14-17]. In the negative detuning regime, or at low temperatures, the polariton-phonon scattering rate is small and it is difficult to attain thermodynamic equilibrium. The system is thus kinetically limited. In contrast, for positive detunings, the increased polariton-phonon scattering rates help to thermalize the lower polaritons (LPs) at $k_{||} \sim 0$ at some effective temperature which can be close to the lattice temperature. However, the critical density for

condensation increases with the increase of positive detuning and temperature. Therefore, there are optimum detunings, or a range of temperatures, for the observation of polariton lasing and for attaining a state close to thermal equilibrium. It is important to note that the LP-LP scattering does not reduce the temperature of the lower polaritons; this is achieved only by LP-phonon scattering.

We had recently reported the strong coupling characteristics of a single GaN nanowire embedded in a dielectric microcavity[9]. The nanowires, grown on silicon, are relatively free of extended defects and the polarization field in them are very small[18-24], leading to a large oscillator strength. The cavity field is mainly within the nanowire region even without additional confinement in the transverse direction. Strong coupling effects characterized by a Rabi splitting of 48 meV have been observed, together with room temperature polariton lasing with an ultra-low optical excitation threshold energy of ~ 93 nJ/cm^2. It is therefore an ideal system to study the effects of exciton-cavity photon detuning on strong coupling and dynamic Bose condensation. In this work, we have investigated the time-integrated momentum distribution and dynamics of polaritons in a single GaN nanowire-dielectric microcavity by angle-resolved and time-resolved spectroscopy. Measurements have been made over the temperature range of 25-100K (a corresponding detuning range of -3.0 to +4.2 meV). Polariton lasing is observed at all temperatures, showing a progression from the kinetic to the thermodynamically controlled regime, with a minimum threshold excitation power at 50K. In terms of dynamic Bose condensation, the best results are observed at 85K with a positive detuning of 2.3 meV. The temperature of the lower polaritons T_{LP} becomes almost equal to the temperature of the lattice T_{latt} and the polariton relaxation time is smaller than the polariton lifetime at $k_{||} \sim 0$ by a factor of 2.

The sample being characterized is a single GaN nanowire of diameter 60 nm and length 750 nm, with the c-axis parallel to the length (growth direction), placed at the central antinode of a dielectric microcavity. The latter consists of a SiO_2 λ-cavity sandwiched by distributed Bragg reflectors (DBRs) on either side consisting of seven pairs of SiO_2/TiO_2 layers. The microcavities that have been investigated are mesa-shaped of 10 μm diameter. A detailed description of the sample and the experimental techniques used for its fabrication have been described elsewhere[9]. Typical micro-photoluminescence spectra from the nanowire before being inserted into the cavity exhibit the three free exciton and the corresponding donor bound (DB) transitions. Of these the exciton X_A and DBX_A are the dominant transitions in the photoluminescence spectrum and therefore the coupling of the X_A exciton to the cavity mode is only considered[9].

The time integrated momentum distribution of the lower polaritons were determined from angle resolved photoluminescence measurements by non-resonant excitation with the linearly polarized emission of a frequency tripled (λ = 267 nm, f_{rep} = 80 MHz and pulse width of 150 fs) Ti:sapphire laser. A doublet lens (with a focal length of 10 cm) was used to focus the incident pump beam from a slant angle of 20º to a spot size of 100 μm on the sample and the emission was collected by a fiber-coupled lens with an angular resolution of 1º and transmitted to a spectrometer. The collection optics was on the extended rails of a goniometer centered at the sample. These measurements were made at temperatures ranging from 25-100K. The spectra at all angles of the out-coupled photon are characterized by a strong LP resonance and a weaker peak corresponding to the upper polariton (UP) (see supplemental material). Using the one-to-one correspondence between the angle of the out-coupled photon and the in-plane wave vector of polaritons, we obtain the energy-momentum distribution of the polaritons. These are shown as false color plots in Fig. 1 at different excitation levels for measurements made at 85K. The

dashed lines represent the dispersion curves obtained from a solution of the coupled harmonic oscillator model considering only the coupling of the X_A exciton and the cavity mode. Values of Rabi splitting Ω_R = 48 meV and detuning δ = +2.3 meV have been used in the analysis. The plots in Fig. 1 reveal that below threshold excitation, the LP emission has a broad distribution both in energy and momentum, whereas above threshold, the emission originates from a condensate formed at $k_{||} \sim 0$ with a linewidth of 0.78 meV and $\Delta k \sim 7x10^3$ cm^{-1} (note that the experimental angular resolution is 1° which corresponds to a $\Delta k \sim 3x10^3$ cm^{-1}). The non-linear optical properties of the nanowire microcavities were also determined from the measured photoluminescence in the normal output direction. A very distinct superlinear increase of the luminescence is observed at the onset of stimulated LP-LP scattering, accompanied by a large decrease in the emission linewidth and a small blueshift of the LP emission peak (see supplemental material). For example, at 70K the linewidth decreases from a maximum of 11 meV to a minimum of 0.58 meV, corresponding to a coherence time of 2.27 ps. The blueshift is 1.83 meV. The threshold polariton density, n_{th}, for the onset of non-linearity derived from the relation $n_{th} = E_{exc}/(E_{pump}D)$ (where D = 60 nm, E_{pump} = 4.64 eV and it is assumed that 100% of the pump photons is absorbed) is plotted in Fig. 2 as a function of detuning. A minimum threshold power density per pulse of 57 nJ/cm^2 (corresponding to a pump power of 0.36 mW) and a corresponding $n_{th} = 1.27x10^{16}$ cm^{-3} per pulse are observed for a negative detuning of δ = -1.3 meV at a temperature of 50K. At large negative detunings, the polariton-phonon scattering rate is small, the relaxation kinetics is insufficient and the threshold is therefore kinetically limited. At the other extreme, in the positive detuning regime, the large polariton effective mass increases the threshold for stimulated scattering and the measured threshold is again high. At the minimum, both kinetics and thermodynamics play an equal limiting role. The calculated critical

densities for the formation of a condensed phase[25-27] in this system at different detunings (temperatures) are shown by the solid curve in Fig. 2. The equation used is:

$$n_c = \frac{1}{S}\sum_{\mu\to 0}\frac{1}{\exp[\frac{E(k)-E(0)-\mu}{k_B T}]} = \frac{1}{(2\pi)^2}\int_{\mu\to 0,\frac{2\pi}{D_S}}^{\infty}\frac{kdk}{\exp[\frac{E(k)-E(0)-\mu}{k_B T}]} \quad (1)$$

where E(k) is the LP energy at wave vector k and E(0) is the energy of the ground state. The chemical potential μ tends to zero. D_S is the size of the system (in this case the microcavity diameter of 10 μm) and $2\pi/D_S$ is the lowest k-state which is $6.3\text{x}10^3$ cm^{-1}. To convert the critical density from 2D to 3D, we have divided by the nanowire diameter.

It is known that the rate of polariton-phonon scattering is dependent on both detuning and temperature[3,17.28]. The effects of the two parameters on polariton-phonon interaction can be separately examined by varying them independently in calculating the scattering rates. For a fixed detuning and a variable temperature, the probability of scattering into the ground state increases with temperature due to an increase in phonon occupation number. Similarly, given a fixed temperature and a variable detuning, the probability of scattering into the ground state is enhanced with increasing detuning by an increase in the exciton fraction of the ground state and the density of states of the LPB. The relative probability of scattering into the ground state is calculated for the two cases. For variable detunings (δ ranging from -3 meV to +4.2 meV and the temperature fixed at 25K), the probability of scattering from a state k into the ground state is calculated relative to the same state at a detuning of -3 meV and is shown in Fig. 3(a). Every k-state is seen to experience an increase in the scattering rate down to the ground state as the

detuning increases, with the state adjacent to the bottom of the LPB experiencing an increase by a factor of ~2 for a positive detuning of +4.2. For variable temperatures (temperature varying from 25K to 100K and δ fixed at -3 meV) the probability of state k scattering to the ground state is calculated relative to the same state at a temperature of 25K and is shown in Fig. 3(b). We see again a monotonic increase in the probability of scattering from every k-state to the ground state as the temperature increases. The enhancement is greatest near the bottom of the LPB, with the state adjacent to the ground state experiencing an increase by a factor of ~ 4 in its scattering rate as the temperature increases from 25K to 100K. The effect of temperature on the kinetics is more pronounced than the effect of detuning, however both parameters are instrumental in the realization of a degenerate condensate in thermal equilibrium. The effects of detuning and temperature on the critical density for condensation were also studied. Figure 3(c) plots the critical density as a function of both detuning (δ ranging from -3 meV to +4.2 meV) and temperature (temperature varying from 25K to 100K). It is evident that the effect of temperature on the critical density in the thermodynamic regime is more pronounced compared to the effect of detuning.

To investigate dynamic condensation in more detail we have first determined the polariton occupancy in k-space as a function of excitation. For this we convert the time-integrated intensity of the angle-resolved LP emission into the number density of LPs by taking into account the $k_{\|}$-dependent density of states and the LP radiative lifetime weighted by the relative photon fraction of the polaritons[29]. It may be noted that in the pulsed excitation scheme used here to avoid sample heating, the polariton temperature and density will change with delay after the excitation. However, in the regime of excitation in which polariton relaxation time is larger than or comparable to the polariton emission time ($P \leq 1.7P_{th}$)[5], the distribution of LP

density in $k_{||}$ - space remains almost invariant. A time-integrated emission intensity from the pulsed measurement is a good approximation for the LP density under these conditions. Far above threshold, the approximation is no longer valid due to the faster polariton dynamics. In Fig. 3(a), the LP number density per k-state at 85K is plotted against energy difference $E - E(k_{||=0})$ for different excitation levels. Below threshold, the scattering mechanisms do not allow for LPs to have enough time to scatter to the ground state and the distribution is non-thermal. At threshold, the kinetics is fast enough and a metastable state is reached wherein the polaritons thermalize via polariton-phonon scattering and which is well described by a Maxwell-Boltzmann (MB) distribution: $N_{MB}(k) = N_0 \exp(-E/k_B T_{LP})$. The solid line is a fit to the data with $N_0 = 1$ and $T_{LP} = 88.8$K. Above threshold, a Bose-Einstein distribution: $N_{BE}(k) = 1/[\exp(E/k_B T_{LP})(1+ N_0^{-1}) - 1]$ describes the data very well except for an occupancy of the condensate at $k_{||} = 0$. The variable T_{LP} and N_0 which are, respectively, the LP temperature and the LP population at $k_{||} = 0$, are used as fitting parameters. The fitting with the BE distribution at $P = 1.3P_{th}$ was achieved with $T_{LP} = 90.2$ K and $N_0 = 3.87$. As the excitation density is increased, T_{LP} increases and this dependence is plotted in the inset of Fig. 3(a). T_{LP} remains constant at ~ 89K upto $1.2P_{th}$, and then increases rapidly. It can be said, with some caution, that with $T_{latt} = 85$K and $T_{LP} = 88.8$K the degenerate polariton condensate is in equilibrium with the phonon bath via dynamic Bose condensation and an optimal balance of kinetics and thermodynamics. However, as the pump rate is increased the LP-phonon scattering is not adequate to cool the polaritons and thermal equilibrium with the phonon bath is not reached any more, though the system can still exhibit polariton lasing. Similar measurements and analysis performed in the temperature range of 25-100K yield the data of Fig. 3(b) and those shown in Table 1. The values of T_{LP} shown in the figure and table reflect excitation levels of $P/P_{th} \approx 1$ where the best fit of the occupancy data is

obtained with a MB distribution. The normalized chemical potential defined as $\alpha = -\mu/k_BT_{LP} = \ln(1+N_0^{-1})$ obtained from the fit of the data of Fig. 3(a) with a MB/BE distribution is plotted in Fig. 3(c) as a function of excitation energy for different detunings. The normalized chemical potential gives insight into the establishment of quantum degeneracy in the system since a quantum degenerate polariton gas in thermal equilibrium is described by a Bose-Einstein distribution with the same temperature as the phonon bath, and with a chemical potential close to zero. Quantum degeneracy is achieved when $N_0 = 1$ and consequently $\alpha = \ln 2 \approx 0.7$. It is seen that the threshold power increases as the detuning increases from negative to positive, in accordance with the data of Fig. 2. It should be noted that all the data points (detunings) of Fig. 2 are not represented in the plots of α in Fig. 3(c). It is interesting to note that the plots of α approximately represent the non-linear polariton lasing behavior as a function of pump power. The quantum degeneracy threshold occurs for $P = P_{th}$ and $N_0 = 1$and a saturation takes place at higher powers due to phase space filling. The plots of measured integrated light intensity versus pump power are shown in the supplemental material.

The dynamic condensation behavior was also studied by performing time-resolved PL (TRPL) measurements using the same pulsed excitation described earlier and detected with a streak camera having an overall system temporal resolution ~5 ps. The transient data recorded at 85K for different excitation powers are shown in Fig. 4(a). The data have been analyzed (as shown in the inset) by a simple two-level rate equation model[15] describing the dynamics between an exciton-polariton reservoir and the LP ground state at $k_{||} \sim 0$. The thermalization time from the hot exciton reservoir down to the ground state is modeled as a single time constant τ_{relax}. Since our objective is to investigate the effect of the interaction of the polaritons with the thermal

phonon bath, we neglect any non-linear time constants and population terms describing the effects of polariton-polariton scattering and stimulated scattering. Accordingly,

$$\frac{dn_R}{dt} = P(t) - \frac{n_R}{\tau_R} - \frac{n_R}{\tau_{relax}} \quad (2)$$

$$\frac{dn_0}{dt} = -\frac{n_0}{\tau_0} + \frac{n_R}{\tau_{relax}} \quad (3)$$

where n_R and n_0 are the reservoir and ground state population, respectively, P(t) is the excitation modeled as a Gaussian pulse and τ_{relax} and τ_0 are scattering time of polaritons from the reservoir to the ground state and the polariton lifetime in the ground state, respectively. The value of τ_0 is fixed and is determined from the cavity Q (~ 600 that corresponds to a photon lifetime τ_{ph} ~ 0.26 ps) and the corresponding photon fraction in the LP branch at the ground state ($\tau_0 = \tau_{ph}/|C_{k||=0}|^2$ and $|C_{k||=0}|$ is determined from the dispersion curves at each temperature). The coupled equations were solved using the non-linear Runge-Kutta technique. Despite the simplicity of the model, the analysis leads to a good fit of the measured data and provides us with a simple insight into the evolution of the thermalization time as a function of pump power. Values of the normalized relaxation time τ_{relax}/τ_0 obtained from the analysis of the data of Fig. 4(a) with the coupled rate equations (1) and (2) are plotted against P/P_{th} for various detunings in Fig. 4(b). While the model of relaxation invoked here is very simplistic, the data exhibited in Fig. 4(b) give some realistic insight to the dynamic condensation process. At low excitation powers polariton relaxation occurs primarily by polariton-phonon scattering and τ_{relax} is large. For all detunings there is a sharp decrease of τ_{relax}/τ_0 at $P/P_{th} \approx 1$which signals the onset of stimulated polariton-polariton scattering and quantum degeneracy at $k_{||} \sim 0$. For the two cases of positive detuning (T = 85 and 100K), $\tau_{relax}/\tau_0 < 1$ at $P = P_{th}$, while it remains larger than unity for T = 70 and 25K (δ = +1.0 and

-3.0 meV). In fact at T = 25K $\tau_{relax}/\ \tau_0$ saturates at a value larger than unity for higher values of P/P_{th}. The polariton-phonon scattering rate is small for negative detuning and τ_{relax} is lowered only by stimulated polariton-polariton scattering, which does not cool the polaritons or lead them towards a state of thermal equilibrium. This only happens for the cases of large positive detuning, and the system is at, or nearly at, thermal equilibrium ($T_{LP} \approx T_{latt}$). Thus, the values and trends of $\tau_{relax}/\ \tau_0$, although obtained from a rather simple model, can give a realistic picture of the dynamic Bose condensation process. Note that we have measured polariton lasing and a distinct non-linear LP luminescence as a function of excitation for all the detuning values. For the case at T = 25K a metastable state and quantum degeneracy are achieved. At the other extreme, for the case at T = 85 and to a lesser extent at T = 100K, the system also attains thermal equilibrium. These observations are in agreement with the data of Fig. 1(d) and 4(b) and Table 1.

In conclusion, we have investigated strong coupling characteristics in a single GaN nanowire-dielectric microcavity over the temperature range of 25 - 100K, which corresponds to an exciton-cavity photon detuning range of -3 to +4.2 meV. Time integrated and time-resolved measurements have been made in this temperature range and the results have been analyzed with appropriate models. Polariton lasing is observed in the entire range of temperature (detuning). The threshold power for the onset of quantum degeneracy, indicated by the onset of non-linear behavior in the lower polariton luminescence goes through a minimum for a detuning δ = -1.3 meV at T = 50K resulting from the interplay of kinetic and thermodynamic limitations to dynamic Bose condensation. It is observed that the polaritons reach equilibrium with the phonon bath, and $T_{LP} \approx T_{latt}$ at T_{latt} = 85K.

The authors acknowledge helpful discussions with H. Deng. The work was supported by the Air Force Office of Scientific Research under Grant FA9550-09-1-0634, and the National Science Foundation (MRSEC Program) under Grant 09-68346.

References

1 C. Weisbuch, M. Nishioka, A. Ishikawa, and Y. Arakawa, *Phys. Rev. Lett.*, **69**, 3314 (1992).

2. G. Khitrova, H.M. Gibbs, F. Jahnke, M. Kira, and S. W. Koch , *Rev. Mod. Phys.*, **71**, 1591 (1999).

3. H. Deng, H. Haug, and Y. Yamamoto, *Rev. Mod. Phys.*, **82**, 1489 (2010).

4. A. Imamoglu, R.J. Ram, S. Pau and Y. Yamamoto, *Phys. Rev. A*, **53**, 4250 (1996).

5. H. Deng, Gregor Weihs, D. Snoke, J. Bloch and Y. Yamamoto, *Proc. Nat. Acad. Sci. USA*, **100**, 15318 (2003).

6. S. Christopoulos, G. Baldassarri Höger von Högersthal, A. J. D. Grundy, P. G. Lagoudakis, A. V. Kavokin, J. J. Baumberg, G. Christmann, R. Butté, E. Feltin, J.-F. Carlin, and N. Grandjean, *Phys. Rev. Lett.*, **98**, 126405 (2007).

7. D. Bajoni, P. Senellart, E. Wertz, I. Sagnes, A. Miard, A. Lemaître, and J. Bloch, *Phys. Rev. Lett.*, **100***,* 047401 (2008).

8. G. Christmann Raphaël Butté, Eric Feltin, Jean-François Carlin, and Nicolas Grandjean, *Appl. Phys. Lett.*, **93**, 051102 (2008).

9. A. Das, J. Heo, M. Jankowski, W. Guo, L. Zhang, H. Deng, and P. Bhattacharya, *Phys. Rev. Lett.*, **107**, 066405 (2011).

10. M. Nomura, N. Kumagai, S. Iwamoto, Y. Ota, and Y. Arakawa, *Nature Physics* **6**, 279 - 283 (2010).

11. J. Kasprzak, M. Richard, S. Kundermann, A. Baas, P. Jeambrun, J. M. J. Keeling, F. M. Marchetti, M. H. Szymańska, R. André, J. L. Staehli, V. Savona, P. B. Littlewood, B. Deveaud and Le Si Dang, *Nature*, **443**, 409 (2006).

12. R. Balili, V. Hartwell, D. Snoke, L. Pfeiffer and K. West, *Science*, **316**, 1007 (2007).

13. H. Deng, Gregor Weihs, D. Snoke, J. Bloch and Y. Yamamoto, *Proc. Nat. Acad. Sci. USA*, **100**, 15318 (2003).

14. G. Malpuech, Y G Rubo, F P Laussy, P Bigenwald and A V Kavokin, *Semicond. Sci. Technol.* **18,** S395–S404 (2003).

15. H. Deng, D. Press, S. Götzinger, G.S. Solomon, R. Hey, K. H. Ploog and Y. Yamamoto *Phys. Rev. Lett.*, **97**, 146402 (2006).

16. J. Kasprzak, D. D. Solnyshkov, R. André, Le Si Dang, and G. Malpuech, *Phys. Rev. Lett.*, **101**, 146404 (2008).

17. J. Levrat R. Butté, E. Feltin, J. Carlin, N. Grandjean, D. Solnyshkov and G. Malpuech, *Phys. Rev. B*, **81,** 125305 (2010).

18. K.A. Bertness, A. Roshko, N.A. Sanford, J.M. Barker, A.V. Davydov, *J. Cryst. Growth*, **287** (2) 522– 527(2006).

19. A. Cavallini, L. Polenta, M. Rossi, T. Stoica, R. Calarco, R. J. Meijers, T. Richter, and H. Lüth *Nano lett.*, **17**(7), 2166 (2007).

20. J. Schlager, K.A. Bertness, P.T. Blanchard, L.H. Robins, A. Roshko, and N.A. Sanford, *J. Appl. Phys.*, **103**, 124309 (2008).

21. C. Chéze, L. Geelhaar, O. Brandt, W.M. Weber, H. Riechert, S. Munch, R. Rothemund, S. Reitzenstein, A. Forchel, T. Kehagias, P. Komninou, G.P. Dimitrakopulos, T. Karakostas *Nano Research*, **3** (7) 528– 536 (2010).

22. W. Guo, M. Zhang, A. Banerjee and P. Bhattacharya *Nano Lett.,* **10** (9), 3355 (2010).

23. W. Guo, A. Banerjee, M. Zhang, and P. Bhattacharya *Appl. Phys. Lett*, **98**, 183116(2011).

24. W. Guo, M. Zhang, P. Bhattacharya, and J. Heo *Nano lett.*, **11** (4), 1434 (2011).

25. J.M..Kosterlitz and D.J. Thouless, *J. Phys. C: Solid StatePhys.* **6** 1181 (1973).

26. D.S. Fisher and P.C. Hohenberg, *Phys. Rev.* B **37** 4938 (1988).

27. Y.E. Lozovik, O.L. Berman, and A.A. Panfinov *Phys.Status Solidi* B **209** 287 (1998).

28. F. Stokker-Cheregi, A. Vinattieri, F. Semond, M. Leroux, I. R. Sellers, J. Massies, D. Solnyshkov, G. Malpuech, M. Colocci, and M. Gurioli, *Appl. Phys Lett.*, **92**, 042119 (2008).

29. The occupation number ($N_{LP}(k_{||})$) is calculated from the intensity ($I_{LP}(k_{||})$) by using the formula, $I_{LP}(k_{||}) = \eta N_{LP}(k_{||}) |C(k_{||})|^2 M/\tau_C$, where η is the collection efficiency, $\tau_C/|C(k_{||})|^2$ is the radiative lifetime of the LPs and M is the number of transverse states subtended by the detection cone. (see *Phys. Rev. Lett.*, **97**, 146402(2006))

Figure Captions:

Figure 1 Polariton dispersion curves at different excitation levels obtained from angle-resolved measurements and displayed as false color plots. The exciton and cavity photon energies are also indiacted. The emission changes from a broad distribution in energy and in-plane momentum space below threshold to a highly localized one above threshold.

Figure 2 Variation of the measured polariton density at threshold and the calculated critical density for the formation of a degenerate condensed phase in the thremodynamic regime, plotted as a function of detuning (temperature).

Figure 3 (a) Polariton-phonon scattering rate to the ground state as a function of in-plane wave vectors for (a) variable detunings at a fixed temperature of 25K calculated relative to the same state at a detuning of -3 meV and (b) variable temperature at a fixed detuning of -3 meV calculated relative to the same state at a temperature of 25K; (c) critical density for condensation calculated in the thermodynamic regime as a function of temperature and detuning.

Figure 4 (a) Occupancy per LP state measured as a function of the energy difference $E_{k||} - E_{k||=0}$. The solid curves indiacte fits obtained with Maxwell-Boltzmann and Bose-Einstein distributions (see text). The inset shows the LP temperature as a function of the incident excitation obtained from the analyses; (b) relative value of LP temperature, with respect to the lattice temperature, as a function of the lattice temperature; (c) dependence of the normalized chemical potential as a function of excitation energy for different detuning values.

Figure 5 (a) Time resolved LP luminescence measured normal to the sample at 85K (δ = 2.3 meV) and at different excitation powers with a resolution of 5 ps. Inset shows the measured transient (normalized) for $P = 1.5P_{th}$ with the calculated values in accordance with the rate equations; (b) normalized relaxation time vs pump power derived from data similar to that of (a) at different temperatures (detunings).

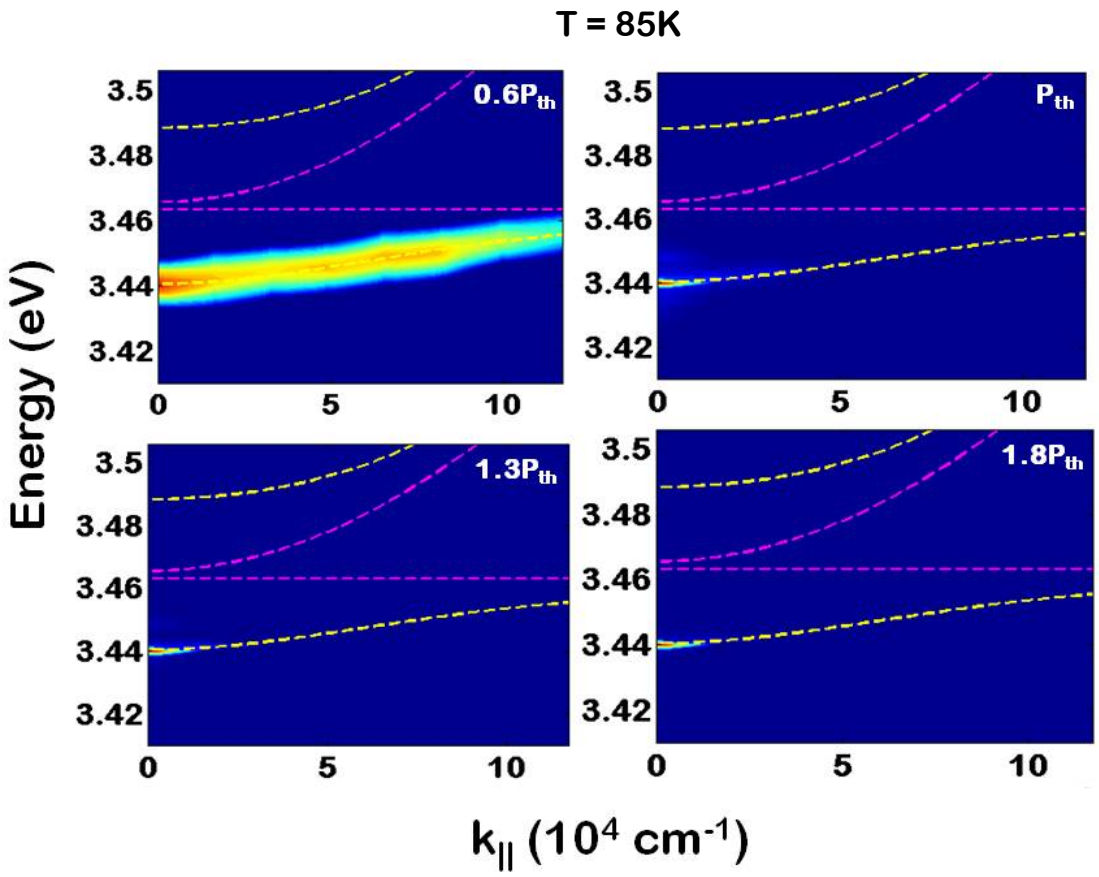

Das *et al.*, Fig. 1 of 5

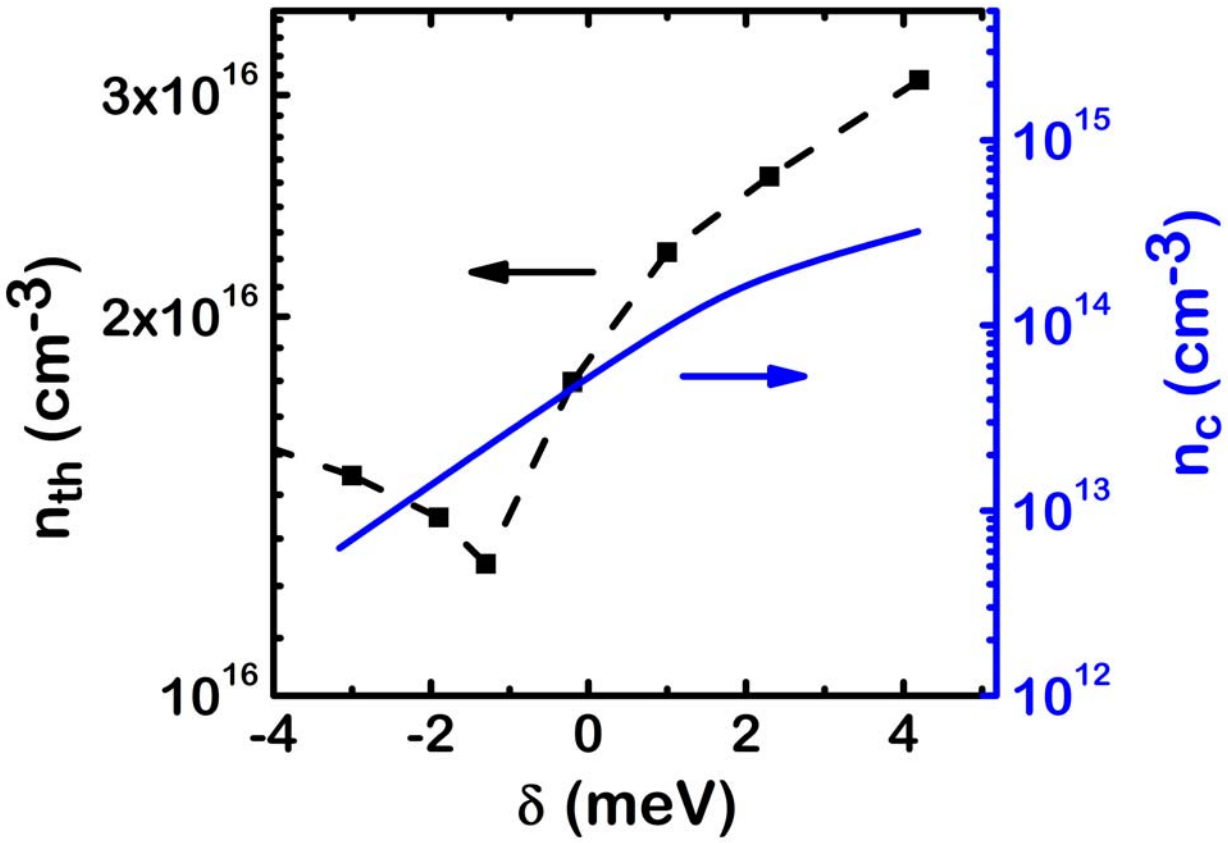

Das *et al.*, Fig. 2 of 5

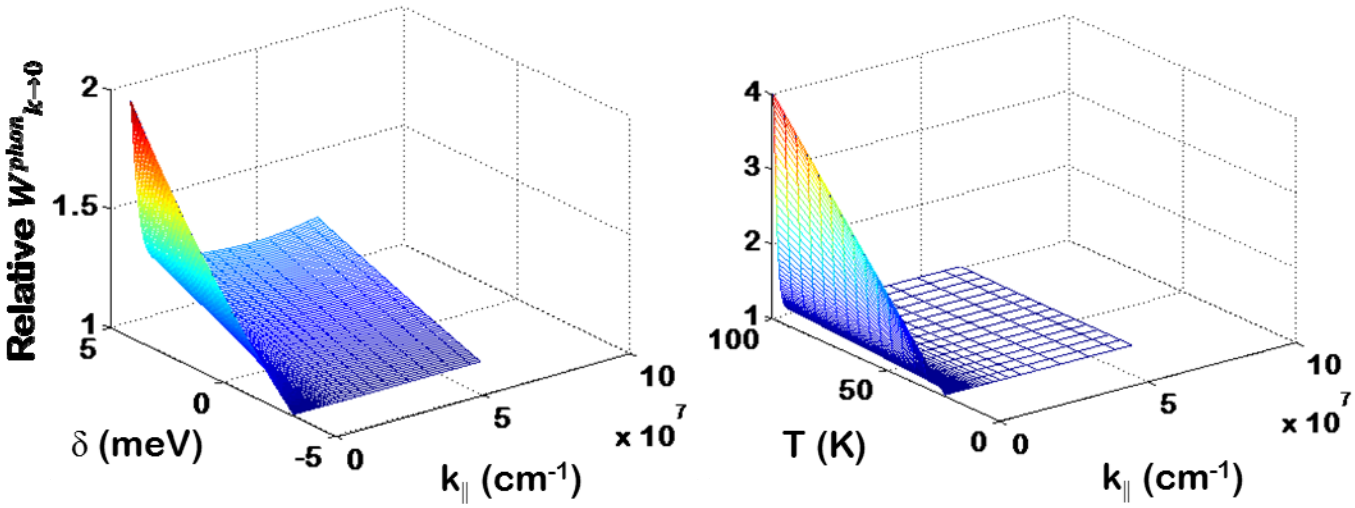

(a) (b)

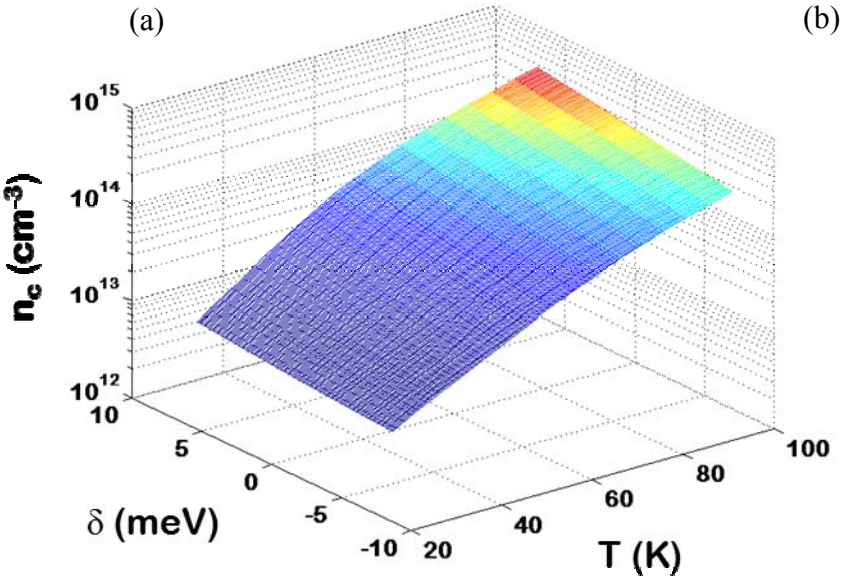

(c)

Das *et al*., Fig. 3 of 5

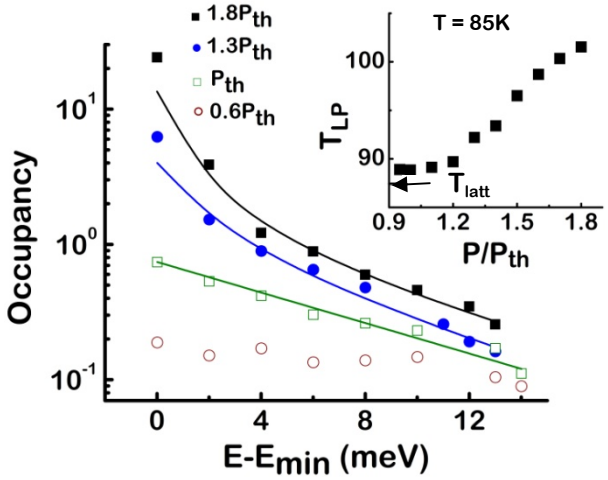

(a)

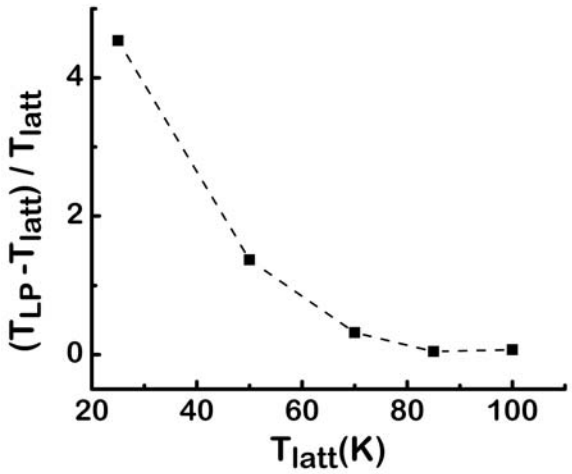

(b)

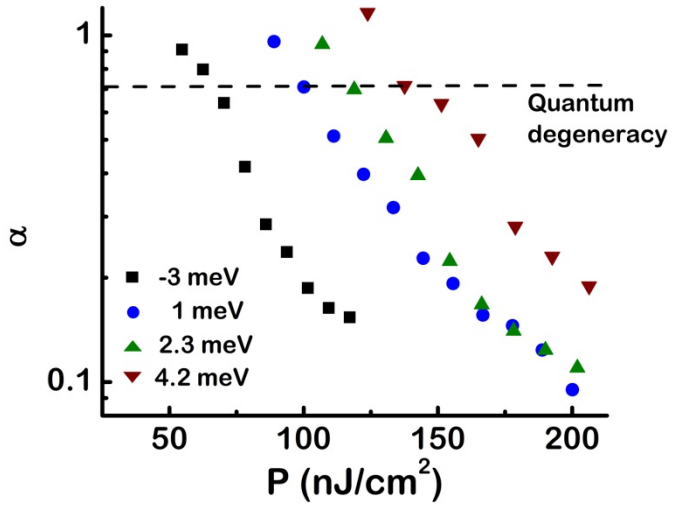

(c)

Das *et al.*, Fig. 4 of 5

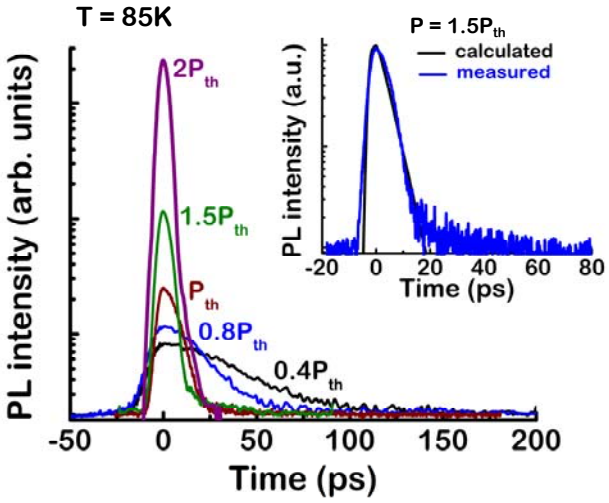

(a)

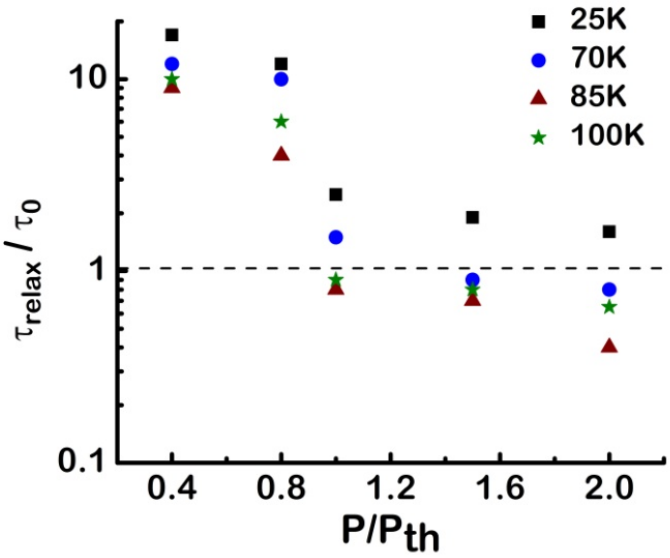

(b)

Das *et al.*, Fig. 5 of 5

TABLE I. Variation of the lower polariton temperature obtained from analysis of occupancy data, with lattice temperature (detuning).

T_{latt} (K)	δ (meV)	T_{LP} (K)	Thermal equilibrium
25	-3	138.46	No
70	1	92.3	No
85	2.3	88.84	Yes
100	4.2	107	Reasonable

Das *et al.*, Table 1 of 1